Three-dimensional instability during vortex merging

Patrice Meunier, Thomas Leweke

Three-dimensional instability during vortex merging

Patrice Meunier† and Thomas Leweke

Institut de Recherche sur les Phénomènes Hors Équilibre,

UMR 6594 CNRS/Universités Aix-Marseille,

49 rue F. Joliot-Curie, F-13384 Marseille Cedex 13, France

Abstract

The interaction of two parallel vortices of equal circulation is observed experimentally. For low Reynolds numbers (Re), the vortices remain two-dimensional and merge into a single one, when their time-dependent core size exceeds approximately 30% of the vortex separation distance. At higher Re, a three-dimensional instability is discovered, showing the characteristics of an elliptic instability of the vortex cores. The instability rapidly generates small-scale turbulent motion, which initiates merging for smaller core sizes and produces a bigger final vortex than for laminar 2D flow.

The merging of two vortices into a single one (also known as 'pairing') has been observed in mixing layers [1], and in the wake of aircraft wings [2–4], and it may play an active role in turbulent flows [5, 6]. In a theoretical study, Saffman and Szeto [7] considered two-dimensional inviscid flow and modeled the vortices as two surfaces of constant vorticity. They found solutions, in which the two patches rotate around each other indefinitely, when their characteristic diameter is smaller than a certain fraction of their separation distance. These solutions are two-dimensionnally linearly [8] and non-linearly [9] stable. Beyond this limit, no such solution exists, and Overman and Zabusky [10] showed numerically that the two patches are rapidly deformed, growing arms of vorticity and merging into a single vortex. Experimental observations made by Griffiths and Hopfinger [11] seem to be in agreement with this size criterion for the evolution of corotating vortex pairs. However, the effect of viscosity, which smoothes the vorticity distribution and makes the core size increase in time, may significantly change this picture. Moreover, the possibility of a three-dimensional instability of the vortex pair has so far not been taken into account. In recent experiments [12], two distinct instabilities have been observed in counterrotating vortex pairs: a long-wavelength instability, treated theoretically by Crow [13], and a short-wavelength instability, identified as the so-called elliptic instability [14–17] of the vortex cores. Whereas a corotating vortex pair was shown theoretically to be stable with respect to long-wavelength perturbations [18], Le Dizès [19] recently predicted the persistence of the short-wavelength instability. A different kind of three-dimensional instability, occurring in columnar corotating vortices, in a rapidly rotating stratified fluid has recently been reported [20]. However, in the absence of stratification and background rotation, the underlying mechanism cannot act in the present flow. In this study, we investigate experimentally the influence of viscous and three-dimensional effects on the merging of two corotating laminar vortices.

The flow is generated in a water tank of dimensions $50 \times 50 \times 130$ cm^3, using two flat plates with sharpened edges, impulsively rotated in a symmetric way by computer-controlled step motors. The vorticity created in the boundary layer of each plate rolls up into two starting vortices, which are laminar, uniform along their axes, and without axial velocity at the

beginning. They are visualized using different dyes, illuminated with laser light in volume or in cross-sections. For quantitative velocity measurements, Particle Image Velocimetry is used. The water is seeded with small reflecting particles and a digital camera captures pairs of images in sections perpendicular to the vortex axes. The images are then treated with a cross-correlation algorithm to extract the velocity and vorticity field [21]. The vortex pair is characterized by the circulation Γ of each vortex, the separation b between the two vortex centers (located at the maxima of vorticity) and the vortex core size a, defined as the radius for which the averaged azimuthal velocity is maximum. Measurements have shown that the initial vorticity distribution of each vortex is approximately Gaussian (see Eq. (1) below).

In this paper, we consider pairs of equal vortices, for which the dynamics depend on two non-dimensional parameters: 1) the Reynolds number $Re = \Gamma/\nu$ (varying between 700 and 4000 here), where ν is the kinematic viscosity of the fluid, and 2) the initial ratio a_0/b_0 of core size and separation distance (initial meaning at the end of the vortex formation), which is in the range 0.1–0.2 in the present experiments. Two point vortices of the same circulation Γ and separated by a distance b_0 rotate around each other by mutual induction (the surrounding fluid being irrotationnal) with a turnover period $t_c = 2\pi^2 b_0^2/\Gamma$. This convective unit is used to non-dimensionalize time t ($t^* = t/t_c$), starting at the beginning of the plate motion.

For Reynolds numbers lower than about 2000, the vortices remain two-dimensional and laminar. They deform elliptically, get closer, and then merge into a single vortex in a rapid transition, as shown by the vorticity fields in Fig. . The distance b between the two maxima of vorticity is plotted in Fig. . The second curve ($Re = 1506$) corresponds to the fields of Fig. . The evolution of the core size a of the two initial vortices before merging, and of the final vortex after merging is shown in Fig. . These measurements reveal that the merging process can be decomposed into several different stages, discussed in the following (the initial phase of vortex roll-up and formation for $t^* < 0.2$ is not considered in further detail in this paper).

In the first stage, the vortices rotate around each other like two point vortices. The

effect of each vortex on the other is weak; it leads to the slight elliptic deformation visible in Fig. (a). The separation distance b remains approximately constant, and the period of rotation is almost equal to the one for a point vortex pair (t_c). The slight oscillation of the separation distance around b_0 is due to the confinement of the flow by the vortex-generating plates, despite the optimization of their motion profile to reduce this effect. The core size a of an axisymmetric vortex with Gaussian vorticity distribution

$$\omega(r) = \frac{\eta\Gamma}{\pi a^2} e^{-\eta r^2/a^2} \tag{1}$$

where $\eta = 1.2563$, solution of the Navier-Stokes equations, grows by viscous diffusion of vorticity according to:

$$a^2 = 4\eta\nu t + const. \tag{2}$$

The solid lines of Fig. correspond to this linear law, which matches the experimentally measured evolution in the first stage of the flow. As the Reynolds number increases, the vortices diffuse slower and this stage lasts longer (in convective time units), as visible in Fig. .

The second stage begins when the vortices reach a critical size, scaled on the separation distance b. At this point, two tips of vorticity are created at the outer side of the vortices (Fig. b), which are subsequently ejected radially to form two arms of vorticity wrapping around the vortices (Fig. c). Meanwhile, the vortex centers get closer and rapidly merge into a single core. The separation distance decreases to zero (see Fig.) within approximately a third of the initial rotation period, an interval which varies little with Reynolds number. This indicates that this second stage, *i.e.* the actual merging, is mainly a convective process, where diffusion of vorticity plays a minor role. For the highest Reynolds number in Fig. , however, the evolution is somewhat slower, because the onset of a three-dimensional instability slightly modifies the merging. During the merging, it is difficult to calculate a core size since the velocity fields of the two vortices strongly interfere.

The critical ratio of core size and separation distance, at which merging begins, is found

experimentally to be (see Fig.):

$$\frac{a_c}{b_0} = 0.29 \pm 0.01. \tag{3}$$

The uncertainty takes into account the error made in the determination of the beginning of merging, which is defined as the time when the separation distance b starts to decrease. This critical ratio is close to the value of 0.32 above which merging of vortex patches is observed, as predicted by theoretical and numerical studies [7, 10]. It is surprising to see that this criterion is little influenced by the initial profile of vorticity, although the definitions of a are necessarily different.

In the third stage, the vorticity arms roll up around the central pattern (Fig. c), forming a spiral of vorticity, which is spread out and smoothed by diffusion (Fig. d). The core size of this final vortex then keeps increasing similarly to the Gaussian evolution (2), although the vortex is not exactly Gaussian after merging. The measurements show, by extrapolation of the viscous core evolutions, that the area of the final vortex is about twice the area of each initial vortex. This increase is larger (beyond measurement uncertainties) than the increase by a factor of $\sqrt{2}$ predicted theoretically by Carnevale *et al.* [22] on the basis of energy and vorticity conservation. In our case with Gaussian vortices, the vorticity seems to decrease during the merging process. This effect, coupled to the conservation of the circulation, leads to an increase of the experimentally measured core size after merging, and may be the explanation for the observed discrepancy.

When increasing the Reynolds number and/or reducing the dimensionless initial core size a_0/b_0, the viscous phase before merging lasts longer, and there is time for a three-dimensional instability to develop while the two vortices are still separated. This phenomenon is here observed for the first time in the corotating vortex pair.

The sideview visualization in Fig. shows a clear observation of the three-dimensional instability. At this particular instant, the vortices, which spin around each other, are in a plane perpendicular to the view direction. The vortex centers are deformed sinusoidally with a wavelength λ close to one vortex separation b, and the perturbations on both vortices

are found to be in phase. This deformation is very similar to what was recently observed in counterrotating vortex pairs [12], where it was found to be a consequence of a cooperative elliptic instability of the vortex cores. It is interesting to see that this instability still develops in a corotating configuration, whereas the long-wavelength instability is suppressed by the rotation of the vortex pair [18]. Elliptic instability occurs in flows with locally elliptic streamlines [14, 16], resulting here from the interaction between the vorticity of one vortex and the external strain induced by the opposite vortex. Theory states that the wavelength scales on the vortex core size a. In our experiment, the most amplified wavelength was measured to be $\lambda/a = 3.1 \pm 0.3$. It is in agreement with the value of 3.5 found for the elliptic instability of a Gaussian vortex in a rotating external strain, which can be derived from theory [19, 17]. This is the first experimental observation of an elliptic instability in such a flow.

Further visualizations and measurements were carried out to determine the growth rate of the instability. By simultaneously illuminating two cross-cut planes B-B and C-C (Fig.), separated by half a wavelength and located at the maximum and minimum of the vortex centerline displacement, one obtains an image as in the inset of Fig. (shown here as a negative). First, these visualizations confirm that the instability mode is stationary (not rotating or propagating) in the rotating frame of reference of the vortex pair, and that the planes of the wavy centerline deformations are aligned with the stretching direction of the mutually induced strain (at 45° with respect to the line joining the vortices), as predicted theoretically [16]. Second, from a series of such images, the amplitude A of the centerline displacement of each vortex can be obtained as function of time. This displacement is proportional to the amplitude of the unstable mode for small values. The result is shown in Fig. . The growth is indeed exponential over a certain period, and an appropriate least-squares fit allows the determination of the growth rate σ. The result corresponding to the straight line of Fig. is:

$$\sigma/\varepsilon = 1.6 \pm 0.2, \tag{4}$$

where $\varepsilon = \Gamma/2\pi b^2$ is the mutually induced external strain at the vortex centers. A theoretical prediction can be obtained, using the results in [19] which extend Baily's theory [15] to the case of an elliptic instability with a rotating strain s, and those in [23] which calculate the value of the strain s at a Gaussian vortex center as a function of the strain far from the center (equal to ε in our experiment). For the present case, with the experimental values of Re and a/b, a growth rate of $\sigma/\varepsilon = 1.757$ is predicted, which is reasonably close to the measured value in (4).

All this evidence indicates that the three-dimensional instability observed in Fig. is indeed an elliptic instability of the strained vortical flow in the cores.

When the perturbation amplitude gets sufficiently large, the organized spatial structure breaks down. At the locations where the vortex centers are most deformed, layers of fluid initially orbiting one vortex are drawn around the respectively other vortex in a periodic interlocking fashion. The corresponding tongues of dye are faintly visible in Fig. . These tongues contain vorticity, which is reoriented and stretched into perpendicular secondary vortices wrapping around the primary pair. This exchange of fluid (and vorticity) between the vortices has two consequences: 1) the vortices are drawn closer together, initiating a premature merging, and 2) the interaction between primary and secondary vortices leads to the almost explosive breakdown of the flow into small-scale motion during this merging. Eventually the flow relaminarizes, and one finds again a single viscous vortex at the end. Despite the 3D perturbation and intermittent turbulence, one can still define effective core sizes. The resulting measurements in Fig. show that merging sets in much earlier, *i.e.* for lower a/b, than in two-dimensional flow (although the actual merging phase may be slightly longer, according to Fig.), and that the final vortex appears to be bigger than it would have been without the three-dimensional instability.

In summary, we have presented experimental results concerning the interaction between two identical, parallel, initially laminar vortices. Unlike for vortices in inviscid flows, merging always happens, since vorticity diffusion makes the vortex core size increase in time, eventually beyond the limit for merging. The evolution of the pair can be decomposed into three

distinct phases: 1) the viscous growth of the cores up to a critical radius of about 30% of the separation distance, 2) the actual merging, *i.e.* the kinematic reorganisation of vorticity into a single core and spiral arms, with little influence of viscosity, and 3) the axisymmetrisation and viscous diffusion of the final vortex, which again depends on Reynolds number. In addition, the measurements show a larger increase in vortex core size during merging than theoretically predicted for inviscid patches. At high Re, a three-dimensional instability is discovered, showing the characteristic features of a cooperative elliptic instability of the vortex cores. The existence of this instability in a situation with rotating external strain is here demonstrated experimentally for the first time. The subsequent stage of small-scale turbulent flow makes the vortices merge for smaller core sizes and into a larger final vortex than in the absence of instability. Experiments are presently underway to quantify in more detail the effect of three-dimensional instability on vortex merging.

REFERENCES

† meunier@marius.univ-mrs.fr

[1] C. D. Winant and F. K. Browand, "Vortex Pairing : the Mechanism of Turbulent Mixing Layer Growth at Moderate Reynolds Number", J. Fluid Mech. **63**(2), 237 (1974).

[2] S. A. Brandt and J. D. Iversen, "Merging of Aircraft Trailing Vortices", J. Aircraft **14**(12), 1212 (1977).

[3] A. L. Chen, J. D. Jacob, and Ö. Savas, "Dynamics of a Corotating Vortex Pairs in the Wakes of Flapped Airfoils", J. Fluid Mech. **378**, 155 (1999).

[4] W. J. Devenport, C. M. Vogel, and J. S. Zsoldos, J. Fluid Mech. **394**, "Flow Structure Produced by the Interaction and Merger of a Pair of Co-rotating Wing-Tip Vortices", 357 (1999).

[5] A. Vincent and M. Meneguzzi, "The Spatial Structures and Statistical Properties of Homogeneous Turbulence" , J. Fluid Mech. **225**, 1 (1991).

[6] O. Cadot, S. Douady, and Y. Couder, "Characterization of the Low Pressure Filaments in Three-Dimensional Turbulent Shear Flow", Phys. Fluids **7**(3), 630 (1995).

[7] P. G. Saffman and R. Szeto, "Equilibrium of a Pair of Equal Uniform Vortices", Phys. Fluids **23**(12), 2339 (1980).

[8] D. G. Dritschel, "The Stability and Energetics of Corotating Uniform Vortices", J. Fluid Mech. **157**, 95 (1985).

[9] D. G. Dritschel, "A Moment Model for Vortex Interactions of the Two-Dimensional Euler Equations. Part 1. Computational Validation of a Hamiltonian Elliptical Representation", J. Fluid Mech. **172**, 157 (1986).

[10] E. A. Overman and N. J. Zabusky, "Evolution and Merger of Isolated Vortex Structures", Phys. Fluids **25**(8), 1297 (1982).

[11] R. W. Griffiths and E. J. Hopfinger, "Coalescing of Geostrophic Vortices", J. Fluid Mech. **178**, 73 (1987).

[12] T. Leweke and C. H. K. Williamson, "Cooperative Elliptic Instability of a Vortex Pair", J. Fluid Mech. **360**, 85 (1998).

[13] S. C. Crow, "Stability Theory for a Pair of Trailing Vortices", AIAA J. **8**(12), 2172 (1970).

[14] C.-Y. Tsai and S. E. Widnall, "The Stability of Short Waves on a Straight Vortex Filament in a Weak Externally Imposed Strain Field", J. Fluid Mech. **73**(4), 721 (1976).

[15] B. J. Baily, "Three-Dimensional Instability of Elliptical Flow", Phys. Rev. Lett. **57**(17), 2160 (1986).

[16] F. Waleffe, "On the Three-Dimensional Instability of Strained Vortices", Phys Fluids *A* **2**, 76 (1990).

[17] C. Eloy and S. Le Dizès, "Three-Dimensional Instability of Burgers and Lamb-Oseen Vortices in a Strain Field", J. Fluid Mech. **378**, 145 (1999).

[18] J. Jiménez, "Stability of a Pair of Co-Rotating Vortices", Phys. Fluids **18**(11), 1580 (1975).

[19] S. Le Dizès, "Three-Dimensional Instability of a Multipolar Vortex in a Rotating Flow",

Phys. Fluids **12**(11), 2762 (2000).

[20] D. G. Dritschel and M. de la Torre Juárez, "The Instability and Breakdown of Tall Columnar Vortices in a Quasi-Geostrophic Fluid" , J. Fluid Mech. **328**, 129 (1996).

[21] M. Raffel, C. Willert, and J. Kompenhans, *Particle Image Velocimetry: a Practical Guide* (Springer-Verlag, 1998).

[22] G. F. Carnevale, J. C. McWilliams, Y. Pomeau, J. B. Weiss, and W. R. Young, "Evolution of Vortex Statistics in Two-Dimensional Turbulence", Phys. Rev. Lett. **66**(21), 2735 (1991).

[23] S. Le Dizès, "Non-Axisymmetric Vortices in Two-Dimensional Flows", J. Fluid Mech. **406**, 175 (2000).

List of figure captions

Figure 1: Vorticity fields during the merging of two corotating vortices for $Re = 1506$ and $a_0/b_0 = 0.18$. (a) $t^* = 0.7$, (b) $t^* = 1.2$, (c) $t^* = 1.6$, (d) $t^* = 2$. Difference between two vorticity contours: $0.3\,\mathrm{s}^{-1}$.

Figure 2: Evolution of the separation distance b for different Reynolds numbers before merging.

Figure 3: Evolution of the square of the core size a before and after merging. Solid lines: evolution for Gaussian vortices. Broken line: $a/b_o = 0.29$.

Figure 4: Side view of the elliptic instability on a corotating vortex pair. $Re = 4140$, $a_0/b_0 \approx 0.15$.

Figure 5: Amplitude of the centerline oscillation. Inset: simultaneous view of the two cross-cut sections B-B and C-C of Fig. (negative image). $Re = 2780$, $\lambda/a = 3.1$.

Figure 6: Evolution of the square of the core size a with and without instability. Broken line: $a/b_o = 0.2$.

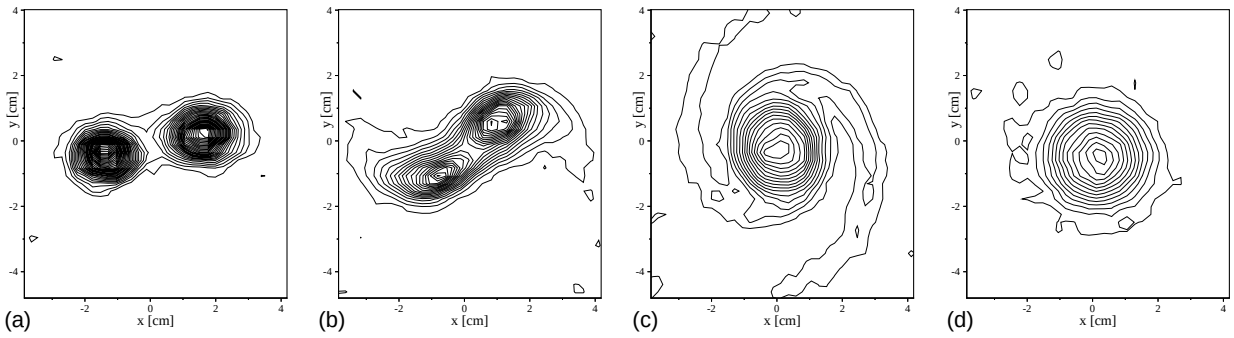

Figure 1, Meunier, Phys. Fluids

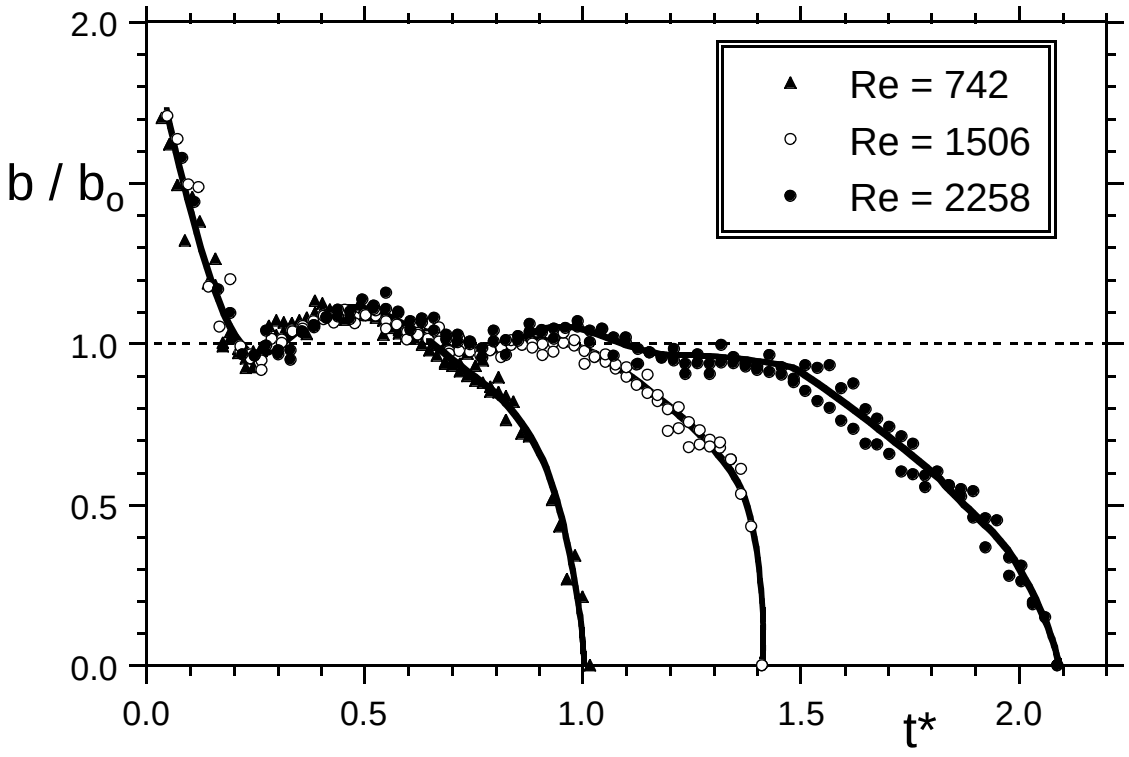

Figure 2, Meunier, Phys. Fluids

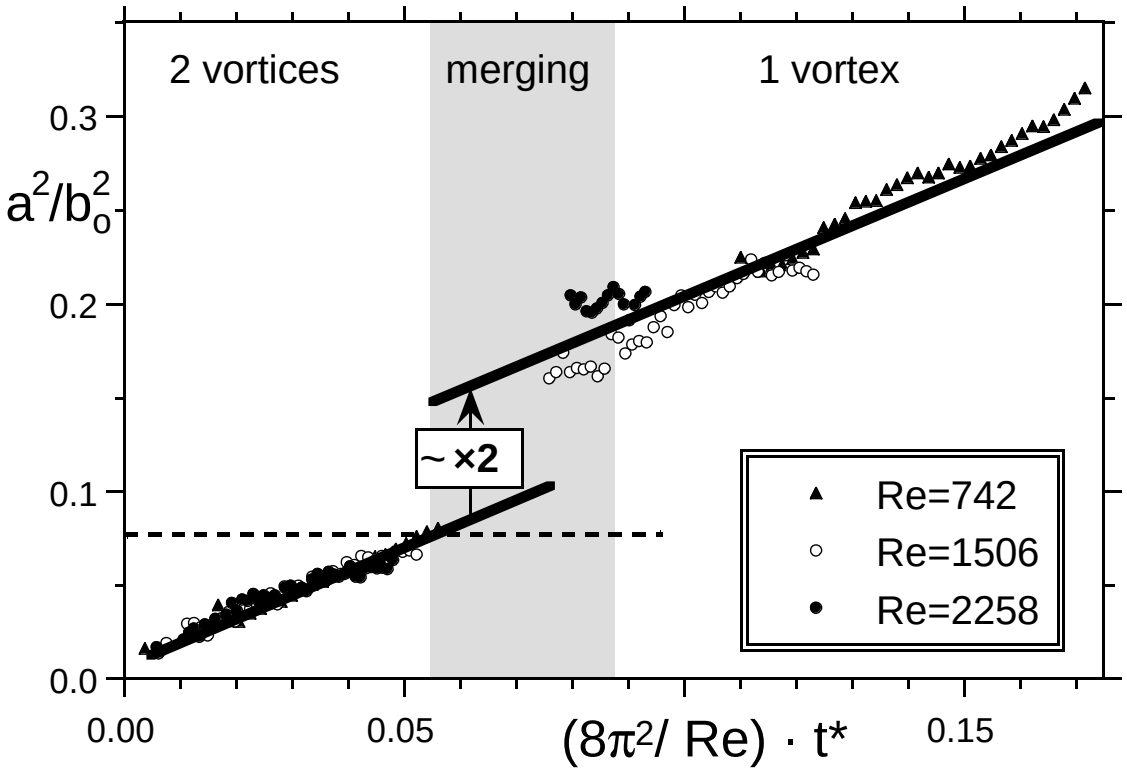

Figure 3, Meunier, Phys. Fluids

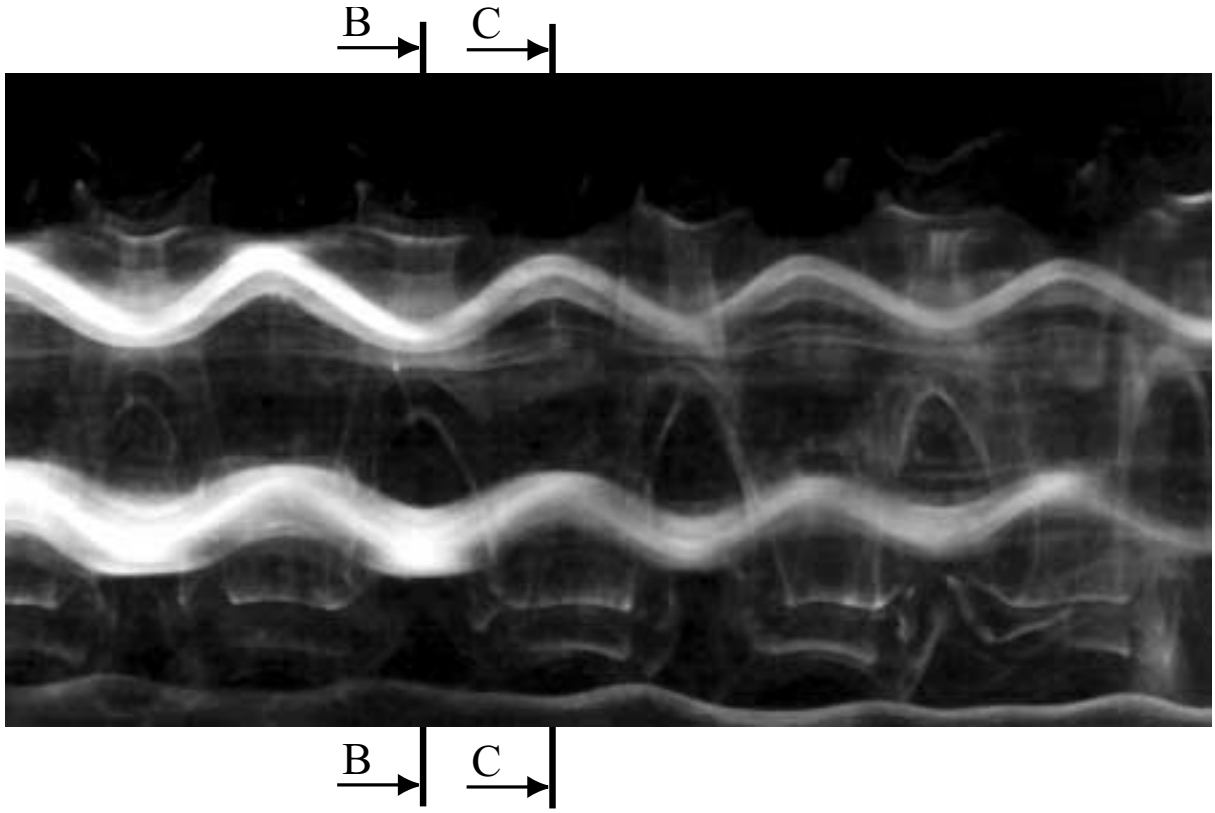

Figure 4, Meunier, Phys. Fluids

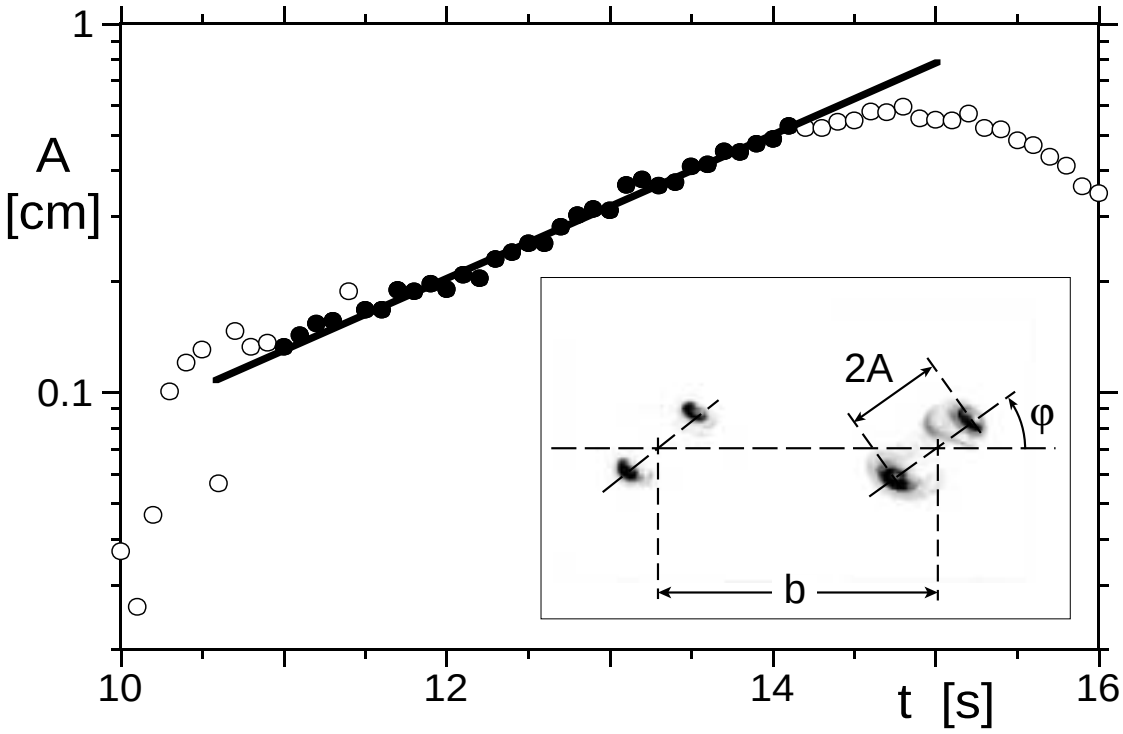

Figure 5, Meunier, Phys. Fluids

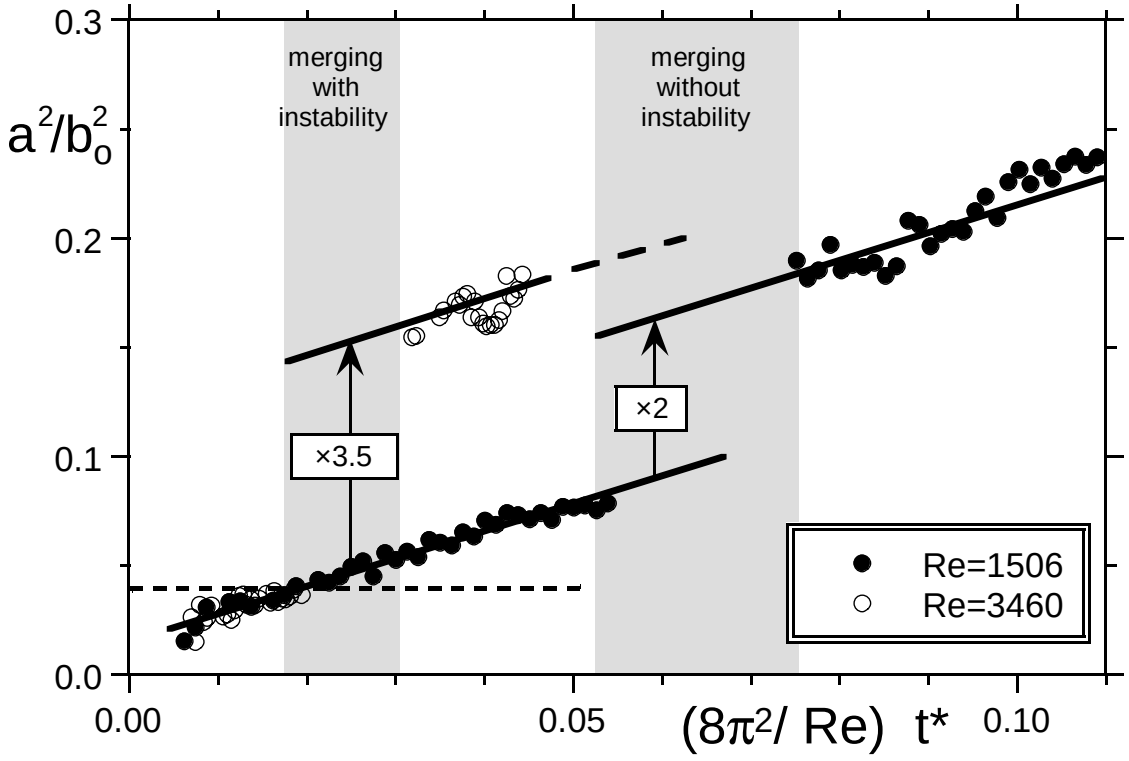

Figure 6, Meunier, Phys. Fluids